inorganics

MDPI

Article

Cysteine Derivatized ^{99m}Tc-Labelled Fatty Acids as β-Oxidation Markers

Theodoros Tsotakos [1], Charalambos Triantis [2], Christos Kiritsis [1], Aggeliki Panagiotopoulou [3], Dimitrios Psimadas [4], Patricia Kyprianidou [1], Maria Pelecanou [3], Minas Papadopoulos [1] and Ioannis Pirmettis [1,*]

1 Institute of Nuclear and Radiological Sciences and Technology, Energy & Safety, NCSR "Demokritos", 15310 Athens, Greece; ttsotakos@gmail.com (T.T.); kiritsis.chr@gmail.com (C.K.); pkypri@rrp.demokritos.gr (P.K.); mspap@rrp.demokritos.gr (M.P.)
2 Department of Pharmacy, Frederick University, Nicosia 1036, Cyprus; hsc.tc@frederick.ac.cy
3 Institute of Biosciences & Applications, NCSR "Demokritos", 15310 Athens, Greece; apanagio@bio.demokritos.gr (A.P.); pelmar@bio.demokritos.gr (M.P.)
4 Department of Nuclear Medicine, University Hospital of Larissa, 41110 Larissa, Greece; dpsimad@gmail.com
* Correspondence: ipirme@rrp.demokritos.gr; Tel.: +30-210-650-3921

Received: 12 September 2019; Accepted: 17 October 2019; Published: 8 November 2019

Abstract: With the aim of developing ^{99m}Tc-labeled fatty acids intended for myocardial metabolism imaging we report herein the synthesis and characterization of two novel derivatives of undecanonoic and hexadecanonoic acid that have been functionalized at the ω-site by cysteine through the formation of a thioether bond (**Cys–FA11** and **Cys–FA16**). Equimolar amounts of each ligand and the $[NEt_4]_2[Re(CO)_3Br_3]$ precursor generated the respective hexacoordinated neutral complexes in which the ligand coordinated to the metal through the SNO donor system of cysteine. The rhenium complexes were characterized by elemental analysis, IR and NMR spectroscopies. The analogous technetium-99m complexes, **^{99m}Tc–Cys–FA11** and **^{99m}Tc–Cys–FA16** were prepared by incubation of the ligand with the precursor $[^{99m}Tc(CO)_3(H_2O)_3]^+$ (radiochemical yield ≥98%). Their structure was established by comparative HPLC techniques. In vivo studies in mice showed high initial heart uptake for both ^{99m}Tc complexes (7.4 ± 0.53 and 7.07 ± 0.73 percentage of injected dose (%ID)/g at 1 min post injection. Rapid clearance (0.60 ± 0.02 %ID/g) was observed for **^{99m}Tc–Cys–FA11** while the clearance of the longer fatty acid **^{99m}Tc–Cys–FA16** was slower (2.31 ± 0.09 %ID/g at 15 min p.i.). Metabolite analysis study indicated that complexes were catabolized through the β-oxidation process.

Keywords: Technetium-99m; rhenium; fatty acid; β-oxidation; radiopharmaceuticals; radiometals

1. Introduction

Fatty acids (FAs) are the main source of energy in normal myocardium providing up to 90% of the energy needed [1]. Once inside the myocardium, where they are transported by passive diffusion or by protein transporters [2], they can either be catabolized through β-oxidation which degrades them by removing two-carbon units, or they can be stored in the form of triglycerides for future use as energy supplies [3]. Under ischaemic conditions oxidation of fatty acids is suppressed and glycolysis and glycogen breakdown are used as an energy source [4]. Therefore, the metabolism of fatty acids and its suppression during ischaemia is a sensitive marker for the normal function of the heart. As a result, the use of radiolabelled fatty acids is considered a valuable diagnostic tool for the detection of ischaemic heart disease, cardiomyopathies and other heart conditions that tamper with cardiac metabolism using either positron emission tomography (PET) or single photon emission computed tomography (SPECT).

^{11}C-Labelled fatty acids are considered the true PET tracers of FAs, however their complicated metabolic profile has prevented wide application [5,6]. The alternatively ^{18}F-labelled fatty acids have presented kinetic differences compared to their unlabelled counterparts that hampered their development [7,8]. Moreover, a major disadvantage for the application of PET tracers is that an on-site cyclotron is required to produce ^{11}C- and ^{18}F-labelled fatty acids [9].

Regarding SPECT radiotracers, one of the earliest and most promising radiotracers of fatty acid metabolism was the 15-(*p*-iodophenyl) pentadecanoic acid (IPPA), which accumulated rapidly in the heart and was cleared with a kinetic profile that resembled that of ^{11}C-palmitate [10–12]. However, due to the rapid washout, quantification of β-oxidation was not possible and image quality was poor. This led to the development of branched-chain analogues of IPPA (Scheme 1), such as the ^{123}I-beta-methyl-*p*-iodophenylpentadecanoic acid (BMIPP) [13–15] which only partially undergoes β-oxidation and is mainly retained in the triglyceride pool. Thus, retention time is increased and image quality is vastly improved [10] rendering BMIPP the radiopharmaceutical of choice for the assessment of cardiac β-oxidation. However, as is the case for all radio-iodinated compounds that must be supplied in a ready to use dosage form, there are logistic problems associated with the production cost and transportation of BMIPP.

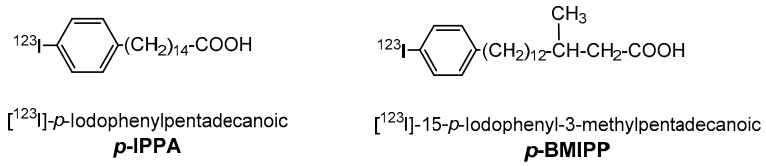

Scheme 1. Structures of iodinated radiopharmaceuticals.

The generator produced ^{99m}Tc is the alternative SPECT radiotracer due to its desirable characteristics ($t_{1/2}$: 6 h, photon energy of 140 keV, widespread availability, low cost). The development of ^{99m}Tc-labelled fatty acids suitable for evaluation of myocardial function and metabolism has been pursued by various research groups since 1975 [16–44]. In all these approaches a chelating moiety has been incorporated into a fatty acid (Scheme 2). Ideally, the moiety should not interfere with the biological properties of the fatty acid allowing recognition by membrane and intracellular proteins [36]. However, the biodistribution studies of the ^{99m}Tc-labelled fatty acids indicated mediocre myocardial uptake, rapid myocardial washout and poor heart/blood and heart/liver ratios when compared to the advantageous biodistribution patterns of the established radio-iodinated fatty acid tracers [16–44].

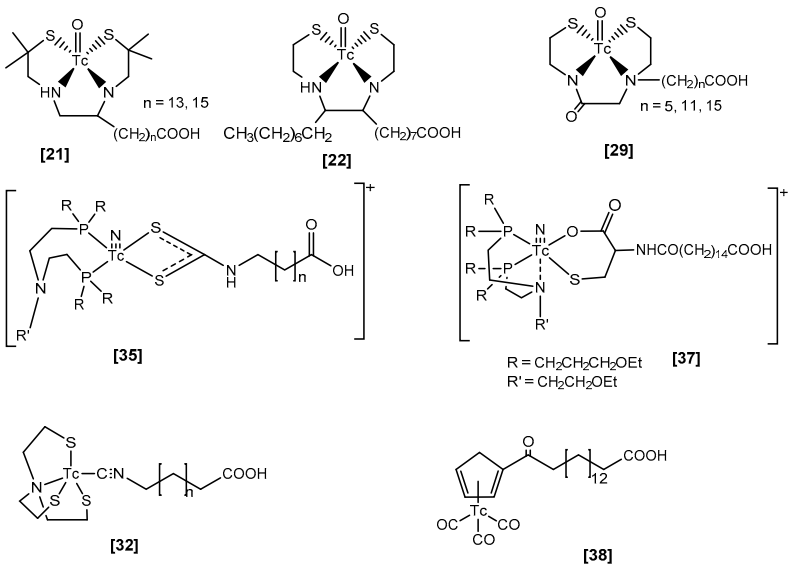

Scheme 2. Selected examples of ^{99m}Tc-labelled fatty acids in different oxidation states [21,22,29,32,35,37,38].

As the chelating moiety used in the synthesis of the ^{99m}Tc-labelled fatty acids plays a prominent role in their biodistribution profile, we report herein the synthesis and characterization of two novel derivatives of undecanoic and hexadecanoic acid with cysteine (**Cys–FA11** and **Cys–FA16** respectively) which acts as a chelator for the $M(CO)_3^+$ core (M = Tc and Re) (Scheme 3). The synthesis, characterization, biodistribution in mice, stability and metabolic studies of their tricarbonyl $^{99m}Tc(CO)_3^+$ complexes, **^{99m}Tc–Cys–FA11** and **^{99m}Tc–Cys–FA16** (Scheme 4), is also reported. For characterization purposes the synthesis of the corresponding $Re(CO)_3^+$ complexes **Re–Cys–FA11** and **Re–Cys–FA16** was effected. Finally, in order to assist in the evaluation of the metabolism data, the analogous complexes with cysteine joined to valeric acid (**Cys–Val**) were also studied.

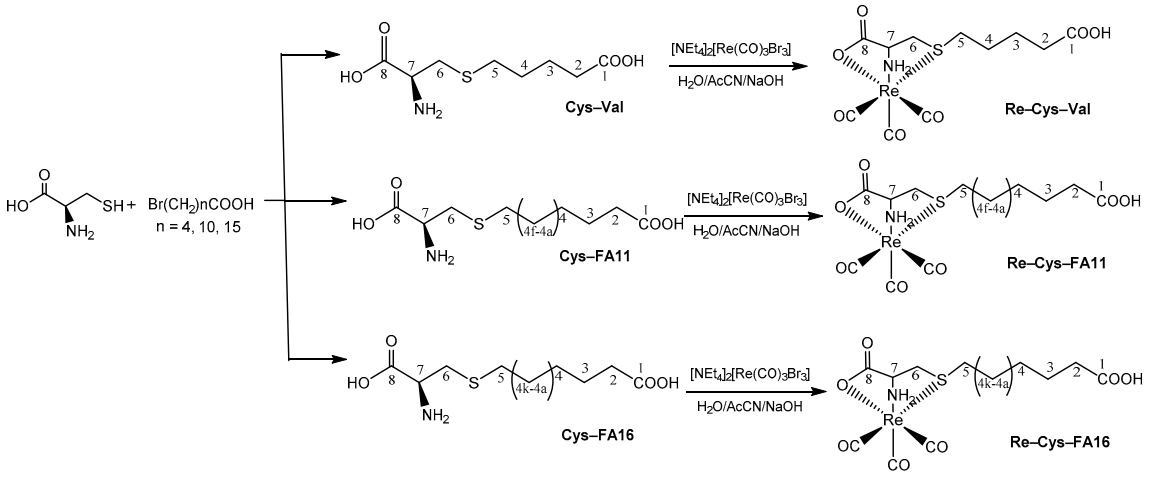

Scheme 3. Synthesis of ligands and rhenium complexes.

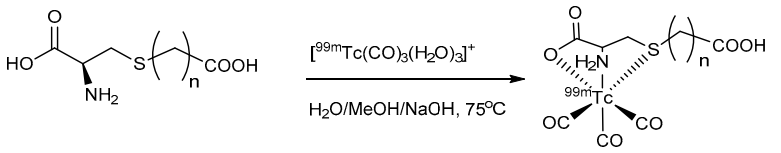

Cys–Val: n = 4
Cys–FA11: n = 10
Cys–FA16: n = 15

^{99m}Tc–Cys–Val: n = 4
^{99m}Tc–Cys–FA11: n = 10
^{99m}Tc–Cys–FA16: n = 15

Scheme 4. Preparation of technetium-99m complexes.

2. Results and Discussion

The cysteine conjugated fatty acid derivatives **Cys–Val**, **Cys–FA11** and **Cys–FA16** (Scheme 1) were synthesized by reacting cysteine with the corresponding ω-bromo fatty acid in alkaline environment and were characterized by elemental analysis, and IR and NMR spectroscopies.

The synthesis of non-radioactive Re(I)-complexes, **Re–Cys–Val**, **Re–Cys–FA11** and **Re–Cys–FA16**, was achieved by ligand exchange reaction using the organometallic Re tricarbonyl precursor $[Net_4]_2[ReBr_3(CO)_3]$ and equimolar quantities of ligands, as shown in Scheme 3. HPLC analysis of reaction mixtures showed in each case the formation of a single peak with retention times 13.6, 19.5 and 22.3 min for **Re–Cys–Val**, **Re–Cys–FA11** and **Re–Cys–FA16** respectively. Complexes were purified with recrystallization and were characterized by elemental analysis and IR and NMR spectroscopies. All complexes were stable in the solid state and in solution as shown by NMR and HPLC for a period of months.

The infrared spectra of all rhenium complexes show strong bands at 1872–2027 cm^{-1} which were attributed to symmetrical and asymmetrical stretches of the C≡O groups of the *fac*-$[Re(CO)_3]^+$ core [45,46]. Characteristic double peaks in the region 2848–2922 cm^{-1} were attributed to C–C stretching of the methylene groups. The complexes also showed strong bands at 1703–1708 cm^{-1} which were due

to C=O stretching of their uncoordinated carboxylate groups, while the CO stretch of their coordinated carboxylates appeared in the 1614–1649 cm^{-1} range.

NMR spectra of all ligands and rhenium complexes were obtained in DMSO-d_6, at 25 °C and assignment was affected through the combined analysis of ^1H–^1H and ^1H–^{13}C correlation spectra (Figures S1–S6). The full ^1H and ^{13}C assignments appear in Tables 1 and 2 while the numbering of the atoms is given in Scheme 3. At room temperature, ^1H and ^{13}C peaks appear broad apparently reflecting the existence in solution of multiple conformations in slow equilibrium.

Table 1. ^1H NMR chemical shift assignments for ligands **Cys–Val**, **Cys–FA11**, **Cys–FA16** and complexes. **Re–Cys–Val**, **Re–Cys–FA11**, **Re–Cys–FA16** in DMSO-d_6 at 25 °C. The numbering of the atoms is given in Scheme 1.

	Cys–Val	**Re–Cys–Val**		**Cys–FA11**	**Re–Cys–FA11**		**Cys–FA16**	**Re–Cys–FA16**
H-2	2.20	2.25	H-2	2.18	2.17	H-2	2.28	2.27
H-3	1.57	1.63	H-3	1.47	1.48	H-3	1.50	1.49
H-4	1.52	1.69	H4, H4a–H4c	1.24	1.25	H4, H-4a–H-4h	1.23	1.25
H-5	2.54	2.90	H-4d	1.24	1.39	H-4i	1.23	1.36
H-6	2.71, 2.97	2.72, 2.89	H-4e	1.32	1.60	H-4j	1.29	1.63
H-7	3.28	4.09	H-4f	1.49	1.50	H-4k	1.49	1.49
NH_2	not visible	6.09, 4.91	H-5	2.54	2.51	H-5	2.53	2.49
OH	not visible	12.01	H-6	2.95, 2.81	2.98, 2.70	H-6	2.98, 2.84	2.87, 2.68
			H-7	3.30	4.10	H-7	3.29	4.09
			NH_2	not visible	6.14, 4.95	OH	8.54	11.83
			OH	not visible	11.82	NH_2	-	6.13, 4.95

Table 2. ^{13}C NMR chemical shift assignments for ligands **Cys–Val**, **Cys–FA11**, **Cys–FA16** and complexes. **Re–Cys–Val**, **Re–Cys–FA11**, **Re–Cys–FA16** in DMSO-d_6 at 25 °C. The numbering of the atoms is given in Scheme 1.

	Cys–Val	**Re–Cys–Val**		**Cys–FA11**	**Re–Cys–FA11**		**Cys–FA16**	**Re–Cys–FA16**
C-1	174.92	173.96	C-1	174.44	174.37	C-1	173.39	173.32
C-2	33.65	32.87	C-2	33.61	33.54	C-2	33.50	33.18
C-3	23.65	23.21	C-3	24.40	24.35	C-3	24.12	24.33
C-4	28.28	27.07	C4, C4a–C4d	28.41–28.79	28.23–28.59	C-4, C-4a–C-4h	28.92–28.35	28.89–28.56
C-5	30.54	32.04	C-4e	28.05	27.69	C-4i	″	28.34
C-6	33.33	36.22	C-4f	28.58	28.51	C-4j	″	27.73
C-7	53.58	57.62	C-5	30.99	31.66	C-4l	28.81	28.76
C-8	168.77	177.13	C-6	31.13	32.22	C-5	31.15	31.59
C≡O	-	193.36, 195.35	C-7	52.28	56.81	C-6	31.16	32.30
			C-8	168.39	176.96	C-7	52.25	56.98
			C≡O	-	193.23, 195.29	C-8	168.58	177.16
						C≡O	-	195.45, 193.20

″: values are the same as above (28.92–28.35).

In the **Cys–Val** ligand, assignment of the valeric acid moiety is straightforward starting from the H-2 methylene protons adjacent to the valeric acid carboxylate group which appear as a distinct, well-separated from the rest, triplet peak. In the **Cys–FA11** and **Cys–FA16** ligands, the H-2 methylene protons, the neighbouring H-3, as well as protons H-5 adjacent to the cysteine sulphur, were easily distinguished, however, extensive peak overlap precluded the specific assignment of most of the middle methylene carbons and protons of the fatty acid chains.

Upon coordination, downfield shifts of 0.8 ppm were noted in all complexes for the H-7 alpha-proton of cysteine, while coordination did not significantly affect the chemical shifts of the H-6 beta-protons, as previously noted in other cysteine complexes with the tricarbonyl core [46]. In the ^{13}C spectra, downfield shifts were noted upon coordination for the cysteine C-7 alpha-carbon by 4.0–4.7 ppm, and the C-8 carboxylate carbon by approximately 8.5 ppm, while smaller downfield shifts

were noted for the cysteine C-6 beta-carbon (1–3 ppm) and the C-5 carbon adjacent to the cysteine sulphur (0.5–1.5 ppm). In addition, upon coordination the amine protons of cysteine that were invisible in the spectra of the ligands, became visible appearing as two distinct broad peaks at approximately 6.1 ppm and 4.9 ppm, the great chemical shift separation apparently reflecting the asymmetry of the complexes.

The technetium-99m complexes (Scheme 4) were synthesized in high yield and radiochemical purity (>95%) by ligand substitution reaction using the precursor *fac*-[^{99m}Tc(H_2O)$_3$(CO)$_3$] and ligand concentration 10^{-3} M. The identity of the technetium-99m complexes was established by HPLC comparison of their retention time to that of the analogous well characterized rhenium complexes by applying parallel radiometric and photometric detection (Figure 1).

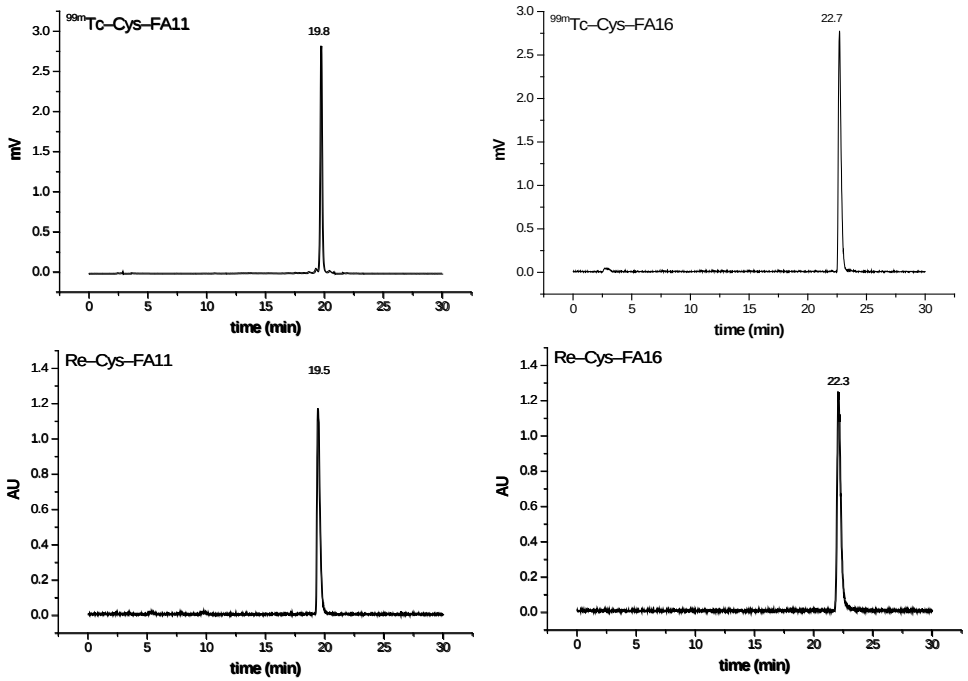

Figure 1. Representative HPLC chromatograms of complexes: **^{99m}Tc–Cys–FA11** and **^{99m}Tc–Cys–FA16** (radiometric detection), **Re–Cys–FA11** and **Re–Cys–FA16** (UV detection).

Lipophilicity studies showed that all complexes were of medium lipophilicity. As expected, complex **^{99m}Tc–Cys–FA16** with the hexadecanoic acid was more lipophilic (Log Do/w 2.24) than complex **^{99m}Tc–Cys–FA11** with the undecanoic acid (Log Do/w 1.018). In vitro stability against transchelation and/or decomposition as determined by the histidine/cysteine challenge study, demonstrated that all complexes were stable against the presence of the two strong tricarbonyl ^{99m}Tc core competitors since after 6 h incubation all complexes remained completely intact.

Human plasma stability studies were performed in order to determine whether plasma proteins bound the radiolabelled complexes and also whether the complexes remained stable after incubation in a biological medium. Results revealed that both complexes remained intact under the employed conditions (≥98%) and were also characterized by low plasma binding, being 38.2% ± 3% for complex **^{99m}Tc–Cys–FA11** and 29.2% ± 4.3% for complex **^{99m}Tc–Cys–FA16** after 2 h incubation (Table 3).

In vivo evaluation of the ^{99m}Tc complexes was carried out in male Swiss Albino mice and the data are presented in Figure 2. The biodistribution study was performed 1 and 15 min after a rapid bolus intravenous injection via the tail vein. Rapid blood clearance was observed for both complexes. The absence of radiation in the stomach and in the spleen indicates the in vivo stability of the complexes in terms of re-oxidation to pertechnetate and TcO_2 respectively. The main excretion route was via the urinary tract for both complexes, and secondary through the hepatobiliary system. The initial heart uptake was similar in both complexes, although slightly lower for the hexadecanoic fatty acid derivative

(7.40 ± 0.53 %ID/g for complex **^{99m}Tc–Cys–FA11** and 7.07 ± 0.73 %ID/g for complex **^{99m}Tc–Cys–FA16**). This finding is consistent with literature reports that correlate myocardial uptake with the length of the fatty acids chain [29,35]. The initial heart uptake values in this study were lower compared to the ^{123}I-IPPA in clinical use (9.51 %ID/g) [37], however, it is comparable to the values of other ^{99m}Tc-labelled fatty acid analogues in mice [27,29,31,37,38,41–44].

Table 3. In vitro protein binding and plasma stability of **^{99m}Tc–Cys–FA11** and **^{99m}Tc–Cys–FA16** at 37 °C.

^{99m}Tc Complexes	Incubation Time	Protein Binding	Stability of ^{99m}Tc Complexes
^{99m}Tc–Cys–FA11	15 min	16.2% ± 1.1%	≥98%
	2 h	38.2% ± 3%	≥98%
^{99m}Tc–Cys–FA16	15 min	13.8% ± 0.6%	≥98%
	2 h	29.2% ± 4.3%	≥98%

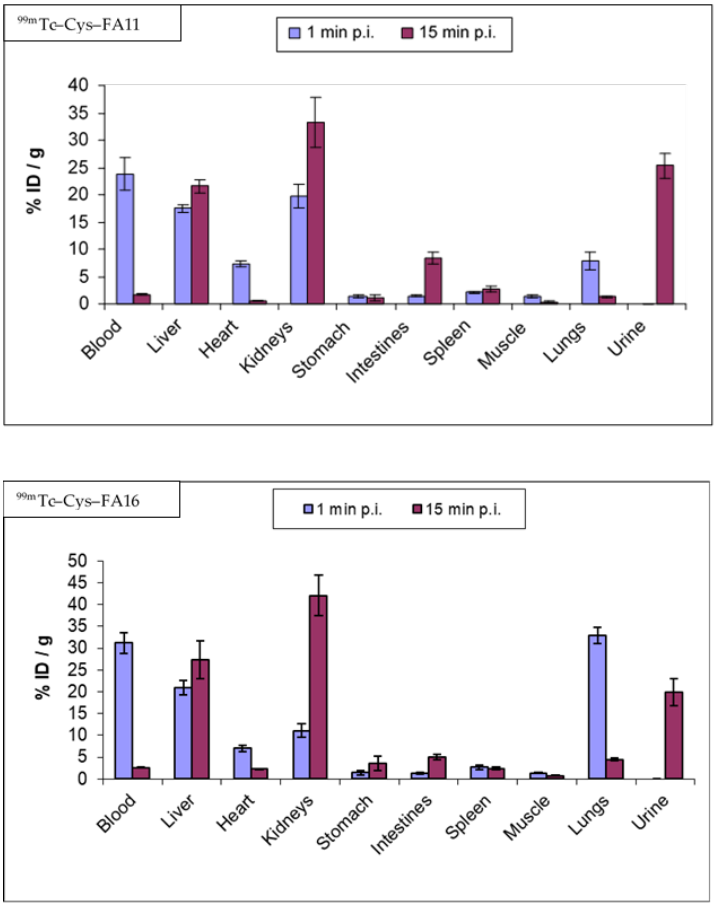

Figure 2. Biodistribution of radioactivity after intravenous injection of **^{99m}Tc–Cys–FA11** and **^{99m}Tc–Cys–FA16** in mice.

The cardiac retention observed for **^{99m}Tc–Cys–FA16** (2.31 ± 0.09 %ID/g) was higher than that observed for **^{99m}Tc–Cys–FA11** (0.60 ± 0.02 %ID/g) at 15 min post injection, possibly due to its longer aliphatic side chain that prolongs metabolism. Despite the favourable profile of the ^{99m}Tc complexes (high radiochemical yield, stability, heart uptake), the key ratios (heart/blood, heart/liver, heart/lungs) were below one for both complexes at all time points studied, a fact that hampers their application as heart metabolism agents without structural modifications.

Metabolite analysis using urine and liver samples was carried out for both radiocomplexes (Figure 3). Urine samples were analysed after a simple filtration through membrane filters, while liver

samples after a process involving homogenization with a mixture of chloroform, methanol and sodium hydroxide, centrifugation and filtration [47]. Most of the radioactivity was extracted in the aqueous fractions (considerably less radioactivity remained in the organic fractions and practically none at the residual pellets formed after centrifugation) and consequently these fractions were analysed by RP-HPLC. Analysis showed the formation of a multitude of radioactivity peaks for both complexes in liver as well as in urine samples. This multitude of radiometabolites was also observed in metabolite analysis of radio-iodinated fatty acid analogues [48–51]. The radiometabolites were more polar than their paternal complexes, as indicated by their retention times, a fact consistent with a catabolisation process through the aliphatic chain of radiolabelled fatty acid analogues. The **^{99m}Tc–Cys–FA11** complex, when catabolized through β-oxidation, should give products with an odd number of carbon atoms in the aliphatic chain, while the **^{99m}Tc–Cys–FA16** complex, should give products with an even number of carbon atoms. RP-HPLC analysis of **^{99m}Tc–Cys–FA11** showed the formation of four main metabolites in liver as well as in urine samples. An assumption would be that these are complexes with three, five, seven and nine carbon atoms in the side chain. This is supported by the fact that the retention time of the metabolite with five carbon atoms in the side chain is exactly the same as the retention time of the well characterized **^{99m}Tc–Cys–Val**. RP-HPLC analysis of **^{99m}Tc–Cys–FA16** showed the formation of seven peaks in liver samples that may belong to seven metabolites with two, four, six, eight, 10, 12 and 14 carbon atoms in the side chain. In urine samples two additional metabolites were observed which may be attributed to the participation of the complex in additional biochemical processes.

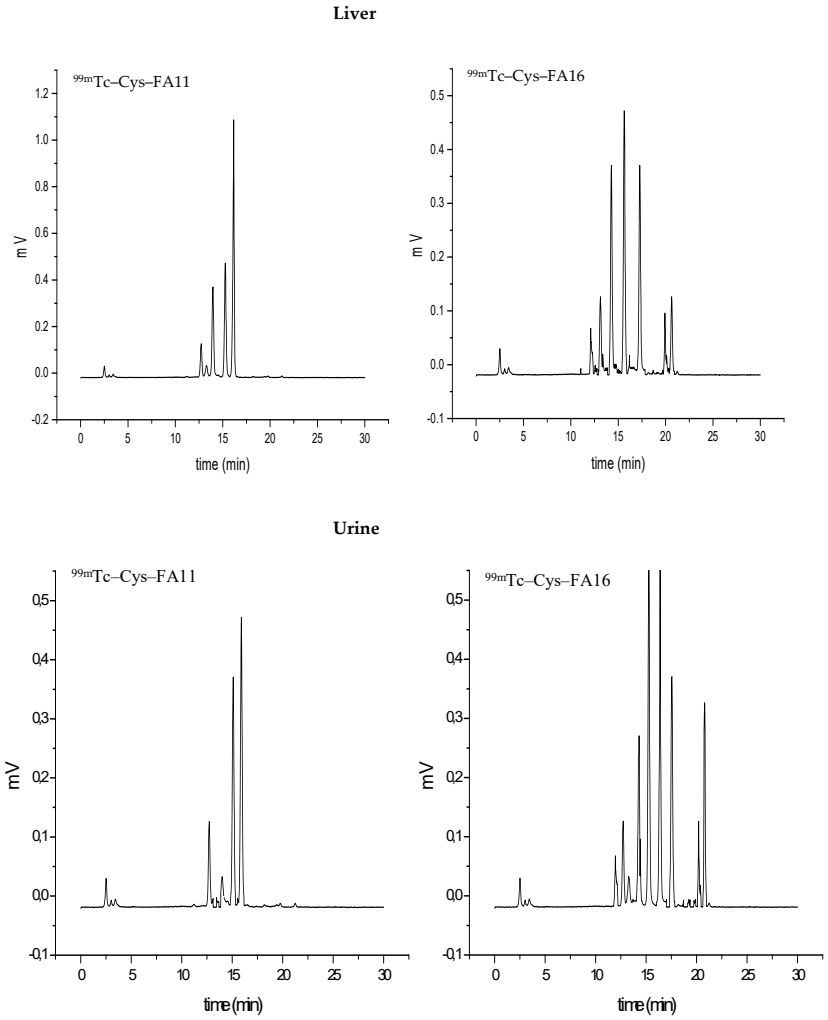

Figure 3. Reverse phase HPLC chromatograms (γ-detection) of liver homogenates and urine analysis 15 min after injection of **^{99m}Tc–Cys–FA11** and **^{99m}Tc–Cys–FA16** in mice.

3. Experimental Section

3.1. Materials and Methods

All laboratory chemicals were reagent grade and were used without further purification. Solvents for high-performance liquid chromatography (HPLC) were HPLC-grade and were filtered through membrane filters (0.22 μm, Millipore, Milford, MA, USA) and degassed by a helium flux before and during use.

IR spectra were recorded on a Nicolet 6700 ATR-IR from Thermo Scientific (Waltham, MA, USA) in the region 4000–500 cm^{-1}. The NMR spectra were recorded in DMSO-d_6, at 25 °C on a Bruker 500 MHz Avance DRX spectrometer (Brucker Biospin, Billerica, MA, USA) using tetramethylsilane (TMS) as internal standard. Elemental analyses for C, H and N were conducted on a Perkin-Elmer 2400 automatic elemental analyser (Perkin Elmer Ltd, Beaconsfield, England). HPLC analysis was performed on a Waters 600 chromatography system coupled to both a Waters 2487 Dual λ absorbance detector and a Gabi gamma detector from Raytest (Elysia-Raytest, Straubenhardt, Germany). Separations were achieved on a Nucleosil C18 (10 μm, 250 mm × 4 mm) column eluted with a binary gradient system at a 1 mL min^{-1} flow rate. Mobile phase A was methanol containing 0.1% trifluoroacetic acid, while mobile phase B was water containing 0.1% trifluoroacetic acid. The elution gradient was 0–1 min 5% A (95% B), followed by a linear gradient to 95% A (5% B) in 15 min; this composition was held for another 15 min. The precursor $[Et_4N]_2[ReBr_3(CO)_3]$ was synthesized according to a literature method [52]. $Na^{99m}TcO_4$ was obtained in physiological saline as a commercial $^{99}Mo/^{99m}Tc$ generator eluate (Mallinckrodt Medical B.V., Petten, The Netherlands). The radioactive precursor *fac*-$[^{99m}Tc(H_2O)_3(CO)_3]^+$ was prepared using a kit containing 5.5 mg of $NaBH_4$, 4 mg of Na_2CO_3, and 20 mg of Na–K tartrate, purged with CO gas, prior to addition of $Na^{99m}TcO_4$, as described in the literature [53].

3.2. Synthesis of 5-((2-Amino-2-Carboxyethyl) Thio) Pentanoic Acid, ***Cys–Val***

Cysteine hydrochloride (1.57 g, 10 mmol) and 5-bromovaleric acid (1.81 g, 10 mmol) were dissolved in 25 mL of 2.5 N aqueous NaOH solution under N_2. The solution was stirred at RT for 24 h, followed by pH adjustment to 5 with glacial acetic acid. The solid formed was collected and recrystallized from methanol [54]. Yield 75%; mp: 209–212 °C. The ^1H and ^{13}C NMR data are given in Tables 1 and 2 respectively. IR: 2915, 2850, 1702 cm^{-1}; elemental analysis: $C_8H_{15}NO_4S$. Calc: C: 43.43, H: 6.83, N: 6.33. Found: C: 43.28, H: 6.95, N: 6.23.

3.3. Synthesis of 11-((2-Amino-2-Carboxyethyl) Thio) Undecanoic Acid, ***Cys–FA11***

Cysteine hydrochloride (1.57 g, 10 mmol) and (2.65 g, 10 mmol) 11-bromoundecanoic acid were dissolved in 25 mL of 2.5 N aqueous NaOH solution under N_2. The solution was stirred at RT for 24 h, followed by pH adjustment to 5 with glacial acetic acid. The solid formed was collected, triturated with hot aqueous methanol (20%) and collected by filtration. Yield 66%; mp: 199–200 °C. The ^1H and ^{13}C NMR data are given in Tables 1 and 2 respectively. IR (cm^{-1}): 2916, 2850, 1704; elemental analysis: $C_{14}H_{27}NO_4S$. Calc: C: 55.05, H: 8.91, N: 4.59. Found: C: 55.20, H: 8.99, N: 4.34.

3.4. Synthesis of 16-((2-Amino-2-Carboxyethyl) Thio) Hexadecanoic Acid, ***Cys–FA16***

Cysteine (600 mg, 4.95 mmol), 16-bromohexadecanoic acid (500 mg, 1.49 mmol), 10 mL 5.4 M sodium methoxide in methanol, and 10 drops of DMSO were added to 170 mL of methanol under N_2. The solution was stirred at RT for 2.5 h followed by the evaporation of the solvent. In the remaining solid, water was added and the pH of the solution was adjusted to pH 5 by the addition of glacial acetic acid. The solid formed was collected by filtration and dried. Yield 64%; m.p.: 215–218 °C. The ^1H and ^{13}C NMR data are given in Tables 1 and 2 respectively. IR: 2915, 2850, 1703 cm^{-1}; elemental analysis: $C_{19}H_{37}NO_4S$. Calc: C: 60.76, H: 9.93, N: 3.73. Found: C: 60.61, H: 10.28, N: 3.61.

3.5. Synthesis of Rhenium Complexes ***Re–Cys–Val***

General method: A mixture of $[NEt_4]_2[ReBr_3(CO)_3]$ (0.2 mmol) and the corresponding ligand (**Cys–Val**, **Cys–FA11**, **Cys–FA16**, 0.2 mmol) dissolved in 5 mL acetonitrile and 1 mL 0.2 N NaOH (0.2 mmol) was refluxed for 2 h. Upon standing at room temperature for 48 h, a pale yellowish product precipitated, collected by filtration and recrystallized from a mixture of methanol/diethylether.

Re–Cys–Val: white powder. Yield 69%, t_R = 13.6 min, IR: 2926, 2851, 2023, 1889, 1705, 1627 cm^{-1}. The ^1H and ^{13}C NMR data are given in Tables 1 and 2 respectively. Elemental analysis: $C_{11}H_{14}NO_7ReS$. Calc: C: 26.94, H: 2.88, N: 2.86. Found: C: 26.78, H: 2.97, N: 2.65.

Re–Cys–FA11: white powder. Yield 58%, t_R = 19.5 min; IR: 2922, 2852, 2022, 1878, 1703, 1614 cm^{-1}. The ^1H and ^{13}C NMR data are given in Tables 1 and 2 respectively. Elemental analysis: $C_{17}H_{26}NO_7ReS$. Calc: C: 35.53, H: 4.56, N: 2.44. Found: C: 35.15, H: 4.79, N: 2.78.

Re–Cys–FA16: yellowish powder. Yield 63%, t_R = 22.3 min, IR: 2915, 2848, 2027, 1872, 1708, 1649 cm^{-1}. The ^1H and ^{13}C NMR data are given in Tables 1 and 2 respectively. Elemental analysis: $C_{22}H_{36}NO_7ReS$. Calc: C: 40.98, H: 5.63, N: 2.17. Found C: 40.67, H: 5.74, N: 1.93.

3.6. Synthesis of ^{99m}Tc Complexes

A freshly prepared solution (400 μL) of the *fac*-$[^{99m}Tc(CO)_3(H_2O)_3]^+$ precursor (pH 8) were added to a vial containing 100 μL of a 5×10^{-3} M aqueous alkaline (pH 8) solution of the cysteine derivatized acids **Cys–Val**, **Cys–FA11** and **Cys–FA16**. The vial was sealed, flushed with N_2 and heated for 30 min at 75 °C. In each case, HPLC analysis demonstrated the formation of a single complex with radiochemical yield >95%. **^{99m}Tc–Cys–Val**: t_R = 13.9 min, **^{99m}Tc–Cys–FA11**: t_R = 19.8 min and **^{99m}Tc–Cys–FA16**: t_R = 22.7 min. Assignment of the structure was based on comparative HPLC studies using the corresponding Re complex as reference.

For all the experiments described below the technetium complexes were isolated by HPLC in order to remove excess ligand and small amounts of radiochemical impurities.

3.7. In Vitro Stability Studies of ^{99m}Tc Complexes

Aliquots of 400 μL of the isolated ^{99m}Tc complexes, **^{99m}Tc–Cys–FA11** and **^{99m}Tc–Cys–FA16**, were added to 100 μL of a 5×10^{-2} M histidine or 5×10^{-2} M cysteine solution in Phosphate Buffer Saline pH 7.4, respectively (final concentration of cysteine and histidine was 10^{-2} M). The samples were incubated for 1, 3 and 6 h at 37 °C and aliquots were removed and analysed by HPLC.

3.8. Plasma Stability

Human blood (~5 mL) was collected in heparinized polypropylene tubes and was centrifuged at 2000 rpm (4 °C) for 15 min and the supernatant (plasma) was collected. Aliquots of the HPLC-purified ^{99m}Tc complexes (100 μL) were incubated at 37 °C with plasma (900 μL). After 15 and 120 min, fractions (450 μL) were withdrawn, mixed with EtOH in a 2:1 EtOH/aliquot *v*/*v* in order to precipitate plasma proteins, and centrifuged at 14,000 rpm for 30 min. Supernatants were filtered and analysed by reverse phase (RP) HPLC.

3.9. Determination of Distribution Coefficient (Log Do/w)

For the evaluation of the lipophilicity of the compounds, the distribution coefficient of the ^{99m}Tc complexes, **^{99m}Tc–Cys–FA11** and **^{99m}Tc–Cys–FA16**, was determined by the shake-flask method. HPLC-purified ^{99m}Tc complexes (10 μL) were mixed with 1.5 mL of 1-octanol and 1.5 mL phosphate buffer (0.125 M, pH 7.4) in a centrifuge tube. The mixture was vortexed at room temperature for 1 min and finally centrifuged at 5000 rpm for 5 min. Three weighed samples from the octanol and aqueous layers were then counted in a gamma counter and the cpm/mL was calculated. Partition coefficient (Log Do/w) was calculated by dividing the cpm/mL (octanol) to cpm/mL (buffer).

3.10. Animal Distribution Studies

Our experimental animal facility is registered according to the Greek Presidential Decree 56/2013 (Reg. Number: EL 25 BIO 022), in accordance to the European Directive 2010/63 which is harmonized with national legislation, on the protection of animals used for scientific purposes. All applicable national guidelines for the care and use of animals were followed. The study protocol was approved by the Department of Agriculture and Veterinary Service of the Prefecture of Athens (Protocol Number: 1606/11-04-2018).

Two groups, each of five Swiss Albino mice (male, 25 ± 3 g), were injected with the HPLC purified ^{99m}Tc complexes, **^{99m}Tc–Cys–FA11** and **^{99m}Tc–Cys–FA16**, (0.1 mL, 1–2 μCi) via the tail vein. The animals were sacrificed by cardiectomy under slight ether anaesthesia at predetermined times (1 and 15 min). The organs of interest were excised, weighed and counted in an automatic gamma counter. Bladder and excreted urine were not weighed. The stomach and intestines were not emptied of food contents prior to radioactivity measurements. The percentage of injected dose per organ (%ID/organ) was calculated by comparison of sample radioactivity to standard solutions containing 10% of the injected dose. The calculation for blood and muscle was based on measured activity, sample weight and body composition data (considering that blood and muscle comprise 7% and 43% of body weight). The percentage of injected dose per gram (%ID/g) was calculated by dividing the %ID/organ by the weight of the organ or tissue. All the animal experiments were carried out in compliance with the relevant national laws relating to the conduct of animal experimentation.

3.11. Metabolites Study

Swiss albino mice were injected with the HPLC purified ^{99m}Tc complexes, **^{99m}Tc–Cys–FA11** and **^{99m}Tc–Cys–FA16**, (0.1 mL, 1–2 mCi) via the tail vein, and liver tissue and urine samples were collected at 15 min post-injection. Liver samples were homogenized in a 2:1:1 mixture of $CHCl_3$, CH_3OH, and 0.001 N NaOH in an automatic homogenizer (Ultra Turrax T25, Janke and Kunkel, IKA-Labortechnik, Staufen, Germany) for 5 min and centrifuged at 14,000 rpm for 30 min [38,47]. The organic and aqueous fractions and residual tissue pellets were counted. Aqueous fractions were filtered through a membrane filter (Millipore, 0.22 μm) and were subsequently analysed by RP-HPLC. Urine samples were analysed by RP-HPLC, after filtration of membrane filters (Millipore, 0.22 μm). The membrane filters were also counted after filtration.

4. Conclusions

In conclusion, the tridentate NSO cysteine ligand was conjugated with an undecanoic and a hexadecanoic acid, to produce two derivatives which coordinated with the *fac*-$[M(CO)_3]^+$ (M = Re, ^{99m}Tc) core through the amine nitrogen, the thioether sulphur and the carboxylate oxygen of the cysteine moiety, forming neutral complexes of medium lipophilicity. The ^{99m}Tc complexes were stable against transchelation in the presence of cysteine and histidine. The complexes also displayed stability in plasma, and a relatively low binding with plasma proteins. Both complexes displayed heart uptake comparable to that of other ^{99m}Tc-labeled fatty acids. Metabolite analysis indicated that complexes were catabolised through the β-oxidation process. In agreement with the involvement of the complexes in β-oxidation metabolic cycles, the heart retention of complex **^{99m}Tc–Cys–FA16** bearing the longer fatty acid chain was longer compared to **^{99m}Tc–Cys–FA11**. Even though the key biodistribution ratios displayed by the complexes precludes their use for the assessment of fatty acid metabolism in the heart, they could serve as a base for structural modifications. In addition, they could be further evaluated as β-oxidation markers in other organs, like the liver.

Supplementary Materials: The following are available online at http://www.mdpi.com/2304-6740/7/11/133/s1, Figure S1: HSQC spectrum of **Re–Cys–Val**, Figure S2: HSQC spectrum of **Re–Cys–FA11**, Figure S3: HSQC spectrum of **Re–Cys–FA16**, Figure S4: COSY spectrum of **Re–Cys–Val**, Figure S5: COSY spectrum of **Re–Cys–FA11**, Figure S6: COSY spectrum of **Re–Cys–FA16**.

Author Contributions: Conceptualization, T.T., M.P. (Maria Pelecanou), M.P. (Minas Papadopoulos), I.P.; investigation, T.T., C.T., C.K., A.P., D.P., P.K.; writing—original draft preparation, T.T.; writing—review and editing, T.T., M.P. (Maria Pelecanou), M.P. (Minas Papadopoulos), I.P.; supervision, M.P. (Maria Pelecanou), M.P. (Minas Papadopoulos), I.P.

Funding: We acknowledge support of this work by the project "NCSRD−INRASTES" research activities in the framework of the national RIS3 (MIS 5002559), which is implemented under the "Action for the Strategic Development on the Research and Technological Sector", funded by the Operational Programme "Competitiveness, Entrepreneurship and Innovation" (NSRF 2014-2020) and cofinanced by Greece and the European Union (European Regional Development Fund).

Conflicts of Interest: The authors declare no conflict of interest.

References

1. Yoshinaga, K.; Tamaki, N. Imaging myocardial metabolism. *Curr. Opin. Biotechnol.* **2007**, *18*, 52–59. [CrossRef]
2. Milger, K.; Herrmann, T.; Becker, C.; Gotthardt, D.; Zickwolf, J.; Ehehalt, R.; Watkins, P.A.; Stremmel, W.; Fullekrug, J. Cellular uptake of fatty acids driven by the ER-localized acyl-CoA synthetase FATP4. *J. Cell Sci.* **2006**, *119*, 4678–4688. [CrossRef]
3. Tamaki, N.; Morita, K.; Kuge, Y.; Tsukamoto, E. The Role of Fatty Acids in Cardiac Imaging. *J. Nucl. Med.* **2000**, *41*, 1525–1534.
4. Heintz, A.C.; Jung, C.M.; Stehr, S.N.; Mirtschink, P.; Walther, M.; Pietzsch, J.; Bergmann, R.; Pietzsch, H.J.; Spies, H.; Wunderlich, G.; et al. Myocardial uptake and biodistribution of newly designed technetium-labelled fatty acid analogues. *Nucl. Med. Commun.* **2007**, *28*, 637–645. [CrossRef]
5. Eckelman, W.C.; Babich, J.W. Synthesis and validation of fatty acid analogs radiolabeled by nonisotopic substitution. *J. Nucl. Cardiol.* **2007**, *14*, S100–S109. [CrossRef]
6. Herrero, P.; Gropler, R.J. Imaging of myocardial metabolism. *J. Nucl. Cardiol.* **2005**, *12*, 345–358. [CrossRef]
7. DeGrado, T.R.; Wang, S.; Holden, J.E.; Nickles, R.J.; Taylor, M.; Stone, C.K. Synthesis and preliminary evaluation of (18)F-labeled 4-thia palmitate as a PET tracer of myocardial fatty acid oxidation. *Nucl. Med. Biol.* **2000**, *27*, 221–231. [CrossRef]
8. DeGrado, T.R.; Kitapci, M.T.; Wang, S.; Ying, J.; Lopaschuk, G.D. Validation of 18F-fluoro-4-thia-palmitate as a PET probe for myocardial fatty acid oxidation: Effects of hypoxia and composition of exogenous fatty acids. *J. Nucl. Med.* **2006**, *47*, 173–181. [PubMed]
9. Uehara, T.; Uemura, T.; Hirabayashi, S.; Adachi, S.; Odaka, K.; Akizawa, H.; Magata, Y.; Irie, T.; Arano, Y. Technetium-99m-Labeled Long Chain Fatty Acid Analogues Metabolized by β-Oxidation in the Heart. *J. Med. Chem.* **2007**, *50*, 543–549. [CrossRef] [PubMed]
10. Gropler, R.J. Radionuclide Imaging of Myocardial Metabolism. *Circ. Cardiovasc. Imaging* **2010**, *3*, 211–222.
11. DeGrado, T.R.; Holden, J.E.; Ng, C.K.; Raffel, D.M.; Gatley, S.J. Quantitative analysis of myocardial kinetics of 15-*p*-[iodine-125] iodophenylpentadecanoic acid. *J. Nucl. Med.* **1989**, *30*, 1211–1218. [PubMed]
12. Reske, S.N.; Sauer, W.; Machulla, H.J.; Knust, J.; Winkler, C. Metabolism of 15 (p^{123}I-iodophenyl-) pentadecanoic acid in heart muscle and noncardiac tissues. *Eur. J. Nucl. Med.* **1985**, *10*, 228–234. [CrossRef] [PubMed]
13. Dormehl, I.C.; Hugo, N.; Rossouw, D.; White, A.; Feinendegen, L.E. Planar myocardial imaging in the baboon model with iodine-123-15-(iodophenyl) pentadecanoic acid (IPPA) and iodine-123-15-(iodophenyl)-3-*R*,*S*-methylpentadecanoic acid (BMIPP), using time-activity curves for evaluation of metabolism. *Nucl. Med. Biol.* **1995**, *22*, 837–847. [CrossRef]
14. Ambrose, K.R.; Owen, B.A.; Goodman, M.M.; Knapp, F.F.J. Evaluation of the metabolism in rat hearts of two new radioiodinated 3-methyl-branched fatty acid myocardial imaging agents. *Eur. J. Nucl. Med.* **1987**, *12*, 486–491. [CrossRef] [PubMed]
15. Goodman, M.M.; Kirsch, G.; Knapp, F.F.J. Synthesis and evaluation of radioiodinated terminal *p*-iodophenyl-substituted alpha- and beta-methyl-branched fatty acids. *J. Med. Chem.* **1984**, *27*, 390–397. [CrossRef] [PubMed]
16. Eckelman, W.C.; Karesh, S.M.; Reba, R.C. New compounds: Fatty acid and long chain hydrocarbon derivatives containing a strong chelating agent. *J. Pharm. Sci.* **1975**, *64*, 704–706. [CrossRef] [PubMed]
17. Karesh, S.M.; Eckelman, W.C.; Reba, R.C. Biological Distribution of Chemical Analogs of Fatty Acids and Long Chain Hydrocarbons Containing a Strong Chelating Agent. *J. Pharm. Sci.* **1977**, *66*, 225–228. [CrossRef]

18. Astheimer, L.; Linse, K.H.; Ramamoorthy, N.; Schwochau, K. Synthesis, Characterization and Evaluation of ^{99}Tc/^{99m}Tc DIARS and DMPE Complexes Containing Pentadecanoic Acid. *Nucl. Med. Biol.* **1987**, *14*, 545–553. [CrossRef]
19. Liang, F.H.; Virzi, F.; Hnatowich, D.J. The Use of Diaminodithiol for Labeling Small Molecules with Technetium-99m. *Nucl. Med. Biol.* **1987**, *14*, 63–67. [CrossRef]
20. Bumbalova, A.; Havranek, E.; Harangozo, M.; Krenek, P.; Lubkeova, S. Preparation and biodistribution of ^{99m} Tc-HT_{18}. *J. Radioanal. Nucl. Chem. Lett.* **1991**, *154*, 53–59. [CrossRef]
21. Mach, R.H.; Kung, H.F.; Jungwiwattanaporn, P.; Guo, Y.Z. Synthesis and Biodistribution of a New Class of ^{99m}Tc-labeled Fatty Acid Analogs for Myocardial Imaging. *Nucl. Med. Biol.* **1991**, *18*, 215–226. [CrossRef]
22. Jones, G.S., Jr.; Elmaleh, D.R.; Strauss, H.W.; Fischman, A.J. Synthesis and Biodistribution of a New ^{99m}Technetium Fatty Acid. *Nucl. Med. Biol.* **1994**, *21*, 117–123. [CrossRef]
23. Jones, G.S., Jr.; Elmaleh, D.R.; Strauss, H.W.; Fischman, A.J. 7,10-Bis(2-Mercapto-2-Methyl)Propyl-7,10-Diazapalmitic Acid: A novel, N_2S_2 Ligand For Technetium-99m. *Bioorg. Med. Chem. Lett.* **1996**, *6*, 2399–2404. [CrossRef]
24. Yamamura, N.; Magata, Y.; Arano, Y.; Kawaguchi, T.; Ogawa, K.; Konishi, J.; Saji, H. Technetium-99m-Labeled Medium-Chain Fatty Acid Analogues Metabolized by β-Oxidation: Radiopharmaceutical for Assessing Liver Function. *Bioconjugate Chem.* **1999**, *10*, 489–495. [CrossRef] [PubMed]
25. Jung, C.M.; Kraus, W.; Leibnitz, P.; Pietzsch, H.J.; Kropp, J.; Spies, H. Syntheses and First Crystal Structures of Rhenium Complexes Derived from ω-Functionalized Fatty Acids as Model Compounds of Technetium Tracers for Myocardial Metabolism Imaging. *Eur. J. Inorg. Chem.* **2002**, *2002*, 1219–1225. [CrossRef]
26. Maresca, K.P.; Shoup, T.M.; Femia, F.J.; Burker, M.A.; Fischman, A.; Babich, J.W.; Zubieta, J. Synthesis, characterization, and biodistribution of a Technetium-99m '3+1' fatty acid derivative. The crystal and molecular structures of a series of oxorhenium model complexes. *Inorg. Chim. Acta* **2002**, *338*, 149–156. [CrossRef]
27. Chu, T.; Zhang, Y.; Liu, X.; Wang, Y.; Hu, S.; Wang, X. Synthesis and biodistribution of ^{99m}Tc-carbonyltechnetiumlabeled fatty acids. *Appl. Rad. Isot.* **2004**, *60*, 845–850. [CrossRef]
28. Lee, B.C.; Choe, Y.S.; Chi, D.Y.; Paik, J.Y.; Lee, K.H.; Choi, Y.; Kim, B.T. 8-Cyclopentadienyltricarbonyl ^{99m}Tc 8-Oxooctanoic Acid: A Novel Radiotracer for Evaluation of Medium Chain Fatty Acid Metabolism in the Liver. *Bioconjugate Chem.* **2004**, *15*, 121–127. [CrossRef]
29. Magata, Y.; Kawaguchi, T.; Ukon, M.; Yamamura, N.; Uehara, T.; Ogawa, K.; Arano, Y.; Temma, T.; Mukai, T.; Tadamura, E.; et al. A Tc-99m-Labeled Long Chain Fatty Acid Derivative for Myocardial Imaging. *Bioconjugate Chem.* **2004**, *15*, 389–393. [CrossRef]
30. Mathur, A.; Mallia, M.B.; Subramanian, S.; Banerjee, S.; Kothari, K.; Sarma, H.D.; Venkatesh, M. Synthesis and bio evaluation of a new fatty acid derivative labelled with technetium-99m. *J. Label Compd. Radiopharm.* **2006**, *49*, 1053–1060. [CrossRef]
31. Lee, B.C.; Kim, D.H.; Lee, J.H.; Sung, H.J.; Choe, Y.S.; Chi, D.Y.; Lee, K.H.; Choi, Y.; Kim, B.T. ^{99m}Tc$(CO)_3$-15-[*N*-(Acetyloxy)-2-picolylamino]pentadecanoic Acid: A Potential Radiotracer for Evaluation of Fatty Acid Metabolism. *Bioconjugate Chem.* **2007**, *18*, 1332–1337. [CrossRef] [PubMed]
32. Walther, M.; Jung, C.M.; Bergmann, R.; Pietzsch, J.; Rode, K.; Fahmy, K.; Mirtschink, P.; Stehr, S.; Heintz, A.; Wunderlich, G. Spies, Synthesis and Biological Evaluation of a New Type of ^{99m}Technetium-Labeled Fatty Acid for Myocardial Metabolism Imaging. *Bioconjugate Chem.* **2007**, *18*, 216–230. [CrossRef] [PubMed]
33. Liu, J.; Xue, Q.; Wang, H.; Wang, H.; Wang, D.; Fang, Y.; Zhang, H. Synthesis and bio-evaluation of Tc-99m-labeled fatty acid derivatives for myocardial metabolism imaging. *Appl. Organometal. Chem.* **2016**, *30*, 596–604. [CrossRef]
34. Tsotakos, T.; Tsoukalas, C.; Patsis, G.; Panagiotopoulou, A.; Nikolić, N.; Janković, D.; Djokić, D.; Raptopoulou, C.P.; Terzis, A.; Papagiannopoulou, D.; et al. Benzimidazole derivatives as NSO ligands for the fac-$[M(CO)_3]^+$ (M = Re, ^{99m}Tc). *Inorg. Chim. Acta* **2011**, *377*, 62–68. [CrossRef]
35. Cazzola, E.; Benini, E.; Pasquali, M.; Mirtschink, P.; Walther, M.; Pietzsch, H.J.; Uccelli, L.; Boschi, A.; Bolzati, C.; Duatti, A. Labeling of Fatty Acid Ligands with the Strong Electrophilic Metal Fragment $[^{99m}Tc(N)(PNP)]^{2+}$ (PNP=Diphosphane Ligand). *Bioconjugate Chem.* **2008**, *19*, 450–460. [CrossRef]

36. Mirtschink, P.; Stehr, S.N.; Pietzsch, H.J.; Bergmann, R.; Pietzsch, J.; Wunderlich, G.; Heintz, A.C.; Kropp, J.; Spies, H.; Kraus, W.; et al. Modified "4+1" Mixed Ligand Technetium-Labeled Fatty Acids for Myocardial Imaging: Evaluation of Myocardial Uptake and Biodistribution. *Bioconjugate Chem.* **2008**, *19*, 97–108. [CrossRef]
37. Mathur, A.; Subramanian, S.; Mallia, M.B.; Banerjee, S.; Samuel, G.; Sarma, H.D.; Venkatesh, M. Synthesis and bio-evaluation of a new fatty acid derivative for myocardial imaging. *Bioorg. Med. Chem.* **2008**, *16*, 7927–7931. [CrossRef]
38. Lee, B.C.; Kim, D.H.; Lee, I.; Choe, Y.S.; Chi, D.Y.; Lee, K.H.; Choi, Y.; Kim, B.T. 16-Cyclopentadienyl Tricarbonyl ^{99m}Tc 16-Oxo-hexadecanoic Acid: Synthesis and Evaluation of Fatty Acid Metabolism in Mouse Myocardium. *J. Med. Chem.* **2008**, *51*, 3630–3634. [CrossRef]
39. Mirtschink, P.; Stehr, S.N.; Walther, M.; Pietzsch, J.; Bergmann, R.; Pietzsch, H.J.; Weichsel, J.; Pexa, A.; Dieterich, P.; Wunderlich, G.; et al. Validation of ^{99m}Tc-labeled "4+1" fatty acids for myocardial metabolism and flow imaging Part 1: Myocardial extraction and biodistribution. *Nucl. Med. Biol.* **2009**, *36*, 833–843. [CrossRef]
40. Mirtschink, P.; Stehr, S.N.; Walther, M.; Pietzsch, J.; Bergmann, R.; Pietzsch, H.J.; Weichsel, J.; Pexa, A.; Dieterich, P.; Wunderlich, G.; et al. Validation of ^{99m}Tc-labeled "4+1" fatty acids for myocardial metabolism and flow imaging Part 2. Subcellular distribution. *Nucl. Med. Biol.* **2009**, *36*, 845–852. [CrossRef]
41. Mathur, A.; Mallia, M.B.; Sarma, H.D.; Banerjee, S.; Venkatesh, M. Evaluation of new positively charged 11- and 12-carbon ^{99m}Tc-labeled fatty acid derivatives for myocardial imaging. *J. Label. Compd. Radiopharm.* **2010**, *53*, 580–585. [CrossRef]
42. Mathur, A.; Mallia, M.B.; Sarma, H.D.; Banerjee, S.; Venkatesh, M. Synthesis, radiolabeling and evaluation of a new positively charged ^{99m}Tc-labeled fatty acid derivative for myocardial imaging. *J. Label. Compd. Radiopharm.* **2011**, *54*, 150–156. [CrossRef]
43. Zeng, H.; Zhang, H.; Wu, X.; Chao, F.; Yu, G.; Zhang, L.; Jiang, H.; Liu, H.; Hou, H.; Zhan, H.; et al. Preliminary studies of a novel cyclopentadienyl tricarbonyl technetium-99m fatty acid derivative for myocardical imaging. *J. Label. Compd. Radiopharm.* **2013**, *56*, 1–5. [CrossRef] [PubMed]
44. Zeng, H.; Zhang, H. Synthesis and biological evaluation of fatty acids conjugates bearing cyclopentadienyl-donors incorporated $[^{99m}Tc/Re(CO)_3]^+$ for myocardical imaging. *Eur. J. Med. Chem.* **2014**, *72*, 10–17. [CrossRef] [PubMed]
45. Karagiorgou, O.; Patsis, G.; Pelecanou, M.; Raptopoulou, C.P.; Terzis, A.; Siatra-Papastaikoudi, T.; Alberto, R.; Pirmettis, I.; Papadopoulos, M. (*S*)-(2-(2′-Pyridyl)Ethyl)Cysteamine and (*S*)-(2-(2′-Pyridyl)Ethyl)-D,L-Homocysteine as Ligands for the "*fac*-$[M(CO)_3]^+$" (M = Re, ^{99m}Tc). *Core. Inorg. Chem.* **2005**, *44*, 4118–4120. [CrossRef] [PubMed]
46. Pirmettis, I.; Arano, Y.; Tsotakos, T.; Okada, K.; Yamaguchi, A.; Uehara, T.; Morais, M.; Correia, J.D.G.; Santos, I.; Martins, M.; et al. New $^{99m}Tc(CO)_3$ Mannosylated Dextran Bearing S-Derivatized Cysteine Chelator for Sentinel Lymph Node Detection. *Mol. Pharm.* **2012**, *9*, 1681–1692. [CrossRef]
47. Forch, J.; Less, M.; Sloane-Stanley, G.H. A simple method for the isolation and purification of total lipids from animal tissues. *J. Biol. Chem.* **1957**, *226*, 497–509.
48. Schmitz, B.; Reske, S.N.; Machulla, H.J.; Egge, H.; Winkler, C. Cardiac metabolism of omega-(*p*-iodophenyl)-pentadecanoic acid: A gas-liquid chromatographic-mass spectrometric analysis. *J. Lipid Res.* **1984**, *25*, 1102–1108.
49. Kropp, J.; Ambrose, K.R.; Knapp, F.F., Jr.; Nissen, H.P.; Biersack, H.J. Incorporation of radioiodinated IPPA and BMIPP fatty acid analogues into complex lipids from isolated rat hearts. *Int. J. Radiat. Appl. Instrum.* **1992**, *19*, 283–288. [CrossRef]
50. Eisenhut, M.; Lehmann, W.D.; Sutterle, A. Metabolism of 15-(4′-[^{123}I]iodophenyl)pentadecanoic acid ([^{123}I]IPPA) in the rat heart; identification of new metabolites by high pressure liquid chromatography and fast atom bombardment-mass spectrometry. *Nucl. Med. Biol.* **1993**, *20*, 747–754. [CrossRef]
51. Yamamichi, Y.; Kusuoka, H.; Morishita, K.; Shirakami, Y.; Kurami, M.; Okano, K.; Itoh, O.; Nishimura, T. Metabolism of iodine-123-BMIPP in perfused rat hearts. *J. Nucl. Med.* **1995**, *36*, 1043–1050. [PubMed]
52. Alberto, R.; Egli, A.; Abram, U.; Hegetschweiler, K.; Gramlich, V.; Schubiger, P.A. Synthesis and reactivity of $[NEt_4]_2[ReBr_3(CO)_3]$. Formation and structural characterization of the clusters $[NEt_4][Re_3(\mu_3\text{-}OH)(\mu\text{-}OH)_3(CO)_9]$ and $[NEt_4][Re_2(\mu\text{-}OH)_3(CO)_6]$ by alkaline titration. *J. Chem. Soc. Dalton Trans.* **1994**, 2815–2820. [CrossRef]

53. Alberto, R.; Schibli, R.; Egli, A.; Schubiger, A.P.; Abram, U.; Kaden, T.A. A Novel Organometallic Aqua Complex of Technetium for the Labeling of Biomolecules: Synthesis of $[^{99m}Tc(OH_2)_3(CO)_3]^+$ from $[^{99m}TcO_4]^-$ in Aqueous Solution and Its Reaction with a Bifunctional Ligand. *J. Am. Chem. Soc.* **1998**, *120*, 7987–7988. [CrossRef]
54. Jiracek, J.; Collinsova, M.; Rosenberg, I.; Budesinsky, M.; Protivinska, E.; Netusilova, H.; Garrow, T.A. S-Alkylated Homocysteine Derivatives: New Inhibitors of Human Betaine-Homocysteine S-Methyltransferase. *J. Med. Chem.* **2006**, *49*, 3982–3989. [CrossRef]